Terrestrial Datum Definition Methods in VLBI Global Solutions

Lisa Kern, Hana Krásná, Axel Nothnagel, Johannes Böhm, and Matthias Madzak

Abstract

A *geodetic datum* describes the origin, orientation and scale of a station network, typically with respect to a reference frame. In the analysis process of Very Long Baseline Interferometry (VLBI) observations, the introduction of a *geodetic datum* is inevitable for the determination of precise reference frames and Earth orientation parameters (EOP). In general, several methods of datum definition exist within the VLBI community, including Helmert rendering and the no-net-translation/no-net-rotation (NNT/NNR) approach. While the first introduces conditions with quasi-infinite weight, the NNT/NNR method can be controlled by the selection of formal errors. Evaluations of the CONT17 legacy-1 campaign and a longer time series of IVS 24-hour sessions show that the variance information (formal errors) of the estimated terrestrial reference frames based on the different methods can differ in the mm to almost cm range. Neglecting this issue could lead to potential issues when combining or comparing solutions from different analysis centers.

Keywords

Geodetic datum · Global solution · Reference systems · Very Long Baseline Interferometry (VLBI)

1 Introduction

Very Long Baseline Interferometry (VLBI) observations, which are the difference in arrival time of signals from extragalactic radio sources at radio telescopes on Earth, enable the determination of precise terrestrial (TRF) and celestial reference frames (CRF) as well as of Earth orientation parameters (EOP). Besides inter-technique combination, which combines the advantages of all space-geodetic techniques, e.g., in the realization of the International Terrestrial Reference Frame (ITRF; Altamimi et al. (2022)), VLBI-only global solutions, both single analysis center and combined multi analysis center combinations, are a necessary step for internal quality control and data interpretation. Global solutions are constructed from as many observing sessions as possible. In the context of datum definition, it does not matter whether the global solution is derived from data of a single analysis center alone or by a combination of data from several analysis centers, e.g., the combined solutions by the International VLBI Service for Geodesy and Astrometry (IVS). As an example for a single analysis center product, the most recent VIE2023sx global solution provided by the Vienna IVS analysis center (VIE) consists of over 7300 sessions and over 20 million observations (Kraśná et al. 2023).

For the construction of a global solution, datum-free normal equation systems (NEQs) are stacked. These are derived from single-session analyses and are stored in solution inde-

All the authors contributed equally to this work.

L. Kern (✉) · H. Krásná · A. Nothnagel · J. Böhm · M. Madzak
Department of Geodesy and Geoinformation, TU Wien, Vienna, Austria
e-mail: lisa.kern@tuwien.ac.at; hana.krasna@tuwien.ac.at; axel.nothnagel@tuwien.ac.at; johannes.boehm@tuwien.ac.at; matthias.madzak@tuwien.ac.at

International Association of Geodesy Symposia,
https://doi.org/10.1007/1345_2024_266, © The Author(s) 2024

pendent exchange (SINEX) format. Typically parameters that are time-dependent (e.g., clocks, atmospheric parameters, EOP) are reduced session-wise, whereas global parameters, that are constant over several sessions, are kept in the NEQ system. Subsequently, the NEQ of the sessions are stacked, i.e., common parameters are added, forming one global NEQ system. By the inversion of the global NEQ system, the global parameters (e.g., station coordinates and source positions) and their corresponding variance information can be estimated.

However, since VLBI observations are relative and only describe the network geometry (configuration) of a three-dimensional VLBI station network with no origin or orientation, the global NEQ is singular and hence not yet invertible. The *geodetic datum* contains all the definitions needed (three translations and three rotations) to locate this stiff station network at an origin and with a specific orientation by applying a Helmert transformation. Since VLBI observations rely on the propagation of microwave signals and consequently on the speed of light, no external information on the seventh parameter of this three-dimensional similarity transformation, the scale, is necessary. Note that *transformation* does not, in this case, mean that the form of the network is distorted since we only consider rigid transformations (Nothnagel 2023). Therefore, six datum constraints are introduced in the adjustment process to compensate for the degree of freedom of the VLBI NEQ and to make the NEQ system regular and solvable (*minimum constraints*; Sillard and Boucher (2001)). Hence, this process is often referred to as the *regularization* of the NEQ. In the case of determining a kinematic solution, the transformation model is extended by the rates of the datum parameters, leading to twelve necessary constraints.

Within the VLBI community, different methods of terrestrial datum realization exist, which will be presented in Sect. 2. Differences between the methods lead to results that are in general not identical and could lead to potential issues when comparing results from different VLBI analysis or combination centers. On the basis of two datasets (see Sect. 3), TRFs are computed using different methods and are compared in Sect. 4.

2 Terrestrial Datum Realization

It must be noted that the *geodetic datum* can be introduced in multiple ways and referred to any reference frame. However, in VLBI analysis, the datum is mostly applied using a conventional reference frame (e.g., ITRF). Since the reference frame is assumed to be accurate and only small changes due to potential new and better observations and models are expected, the vectorial residuals $\mathbf{\Delta x}$ of the transformation from the VLBI network frame $\mathbf{x}$ to the reference frame $\tilde{\mathbf{x}}$ should generally be close to zero for most of the stations. However, in the event of earthquakes occurring after an ITRF release, these differences can become significantly large.

Furthermore, usually, a subset of stations is used to define the datum (*partial inner constraints*; Blaha (1971); Dermanis (1994)) which will be referred to as *datum stations*. These stations should have a long observation history and are chosen to provide relatively consistent global coverage. Note that for the sake of simplicity, any usage of $\mathbf{x}$ in the following Sects. 2.1 and 2.2 only refers to station positions and that the NEQ solely carries information for determining these global parameters. As already mentioned, when determining a kinematic reference frame, the transformation model is extended by the rates of the datum parameters. The corresponding equations can be found in Nothnagel (2023).

In general, there are two expressions used in the following, *conditions* strictly force the model onto the VLBI configuration (they have quasi-infinite weight; see Sect. 2.1), whereas *constraints* can be controlled by formal errors, which are used to populate a covariance matrix for the generation of a regular NEQ system (see Sect. 2.2, Eqs. 8, 11).

2.1 Helmert Rendering

The Helmert similarity transformation is a widely used approach to relate two frames by shifting along and rotating around the coordinates axis. The coordinates of the N selected datum stations in the VLBI network frame $\mathbf{x}$ and the coordinates in the reference frame $\tilde{\mathbf{x}}$ are related as follows

$$\tilde{\mathbf{x}} = \begin{pmatrix} 1 & -r_z & r_y \\ r_z & 1 & -r_x \\ -r_y & r_x & 1 \end{pmatrix} \cdot \mathbf{x} + \begin{pmatrix} t_x \\ t_y \\ t_z \end{pmatrix} \tag{1}$$

with t_x, t_y, t_z, r_x, r_y and r_z being the translation t and rotation r parameters. By re-shaping and ordering, the observation equations $\Delta\mathbf{x} = \mathbf{x} - \tilde{\mathbf{x}}$ read

$$\begin{pmatrix} \Delta x_i \\ \Delta y_i \\ \Delta z_i \end{pmatrix} = \begin{pmatrix} 1 & 0 & 0 & 0 & -\tilde{z}_i & \tilde{y}_i \\ 0 & 1 & 0 & \tilde{z}_i & 0 & -\tilde{x}_i \\ 0 & 0 & 1 & -\tilde{y}_i & \tilde{x}_i & 0 \end{pmatrix} \cdot \begin{pmatrix} t_x \\ t_y \\ t_z \\ r_x \\ r_y \\ r_z \end{pmatrix} \quad \rightarrow \quad \mathbf{\Delta x} = \mathbf{B} \cdot \xi. \tag{2}$$

Setting up these equations per datum station i and vertically stacking them, $\mathbf{B}$ is the Jacobi matrix of the Helmert parameters with dimensions $3N \times 6$. Finally, $\mathbf{B}$ is used to render the datum-free normal equation matrix $\mathbf{N}_{free}$, by

the expansion of the NEQ system and forcing the Helmert parameters to be zero ($\xi = 0$).

$$\begin{pmatrix} \mathbf{N}_{free} & \mathbf{B} \\ \mathbf{B^T} & 0 \end{pmatrix} \begin{pmatrix} \mathbf{\Delta x} \\ \xi = 0 \end{pmatrix} = \begin{pmatrix} \mathbf{b_{free}} \\ 0 \end{pmatrix} \tag{3}$$

The corresponding covariance matrix of the estimated parameters is

$$\mathbf{C}_{\mathbf{x},HR} = \sigma^2 \mathbf{N}_{free}^{-1} \tag{4}$$

with σ^2 being the a posteriori variance of unit weight. The subscript *HR* denotes the method, Helmert rendering. This is the classical way of adding conditions to the adjustment, also known as *Gauss-Markov model with restrictions/conditions*.

2.2 NNT/NNR

A currently widely used approach includes the introduction of no-net-translation (NNT) and no-net-rotation (NNR) constraints (see Eqs. 5 and 6 respectively) to N datum stations, which are used to map a set of telescopes to a conventional reference set. $\mathbf{r}$ represents the position vector in Cartesian three-dimensional coordinates.

$$\sum_{i=1}^{N} \mathbf{\Delta x} = \sum_{i=1}^{N} \begin{pmatrix} \Delta x_i \\ \Delta y_i \\ \Delta z_i \end{pmatrix} = \begin{pmatrix} 0 \\ 0 \\ 0 \end{pmatrix} \tag{5}$$

$$\sum_{i=1}^{N} (\mathbf{r} \times \mathbf{\Delta x}) = \sum_{i=1}^{N} \left(\begin{pmatrix} \tilde{x}_i \\ \tilde{y}_i \\ \tilde{z}_i \end{pmatrix} \times \begin{pmatrix} \Delta x_i \\ \Delta y_i \\ \Delta z_i \end{pmatrix} \right) = \begin{pmatrix} 0 \\ 0 \\ 0 \end{pmatrix} \tag{6}$$

By forming the partial derivatives of the translation and rotation constraints, they can be combined into one composite constraint

$$\sum_{i=1}^{N} \begin{pmatrix} 1 & 0 & 0 \\ 0 & 1 & 0 \\ 0 & 0 & 1 \\ 0 & -\tilde{z}_i & \tilde{y}_i \\ \tilde{z}_i & 0 & -\tilde{x}_i \\ -\tilde{y}_i & \tilde{x}_i & 0 \end{pmatrix} \cdot \begin{pmatrix} \Delta x_i \\ \Delta y_i \\ \Delta z_i \end{pmatrix} = \mathbf{0} \;\rightarrow\; \sum_{i=1}^{N} \mathbf{B}^T \cdot \mathbf{\Delta x} = \mathbf{0} \tag{7}$$

leading to the constraint matrix $\mathbf{B}$ with dimensions $3N \times 6$ which is a vertically concatenated matrix of the individual B_i values and is used to resolve the rank defect of the datum-free normal equation matrix $\mathbf{N}_{free}$. When comparing the condition/constraint matrices from Eq. 2 (Helmert rendering) and Eq. 7 (NNT/NNR), it can be noted that they are identical and should lead to the same results. However, as stated in the beginning, in comparison to the Helmert rendering, it is possible to incorporate formal errors for the constraints. Hence, a covariance matrix $\mathbf{\Sigma}$ with dimensions 6×6, which specifies the impact of datum constraints on the solution, is applied to generate a regular normal equation matrix forming the datum matrix $\mathbf{N}_B$, whereas the right-hand side vector of the datum $\mathbf{b}_B$ is zero:

$$\mathbf{N}_B = \mathbf{B}\mathbf{\Sigma}^{-1}\mathbf{B}^T. \tag{8}$$

The datum matrix can also be determined in another way by forming the solution equation for the transformation parameters ξ

$$\xi = (\mathbf{B}^T\mathbf{B})^{-1}\mathbf{B}^T\mathbf{\Delta x} \tag{9}$$

and imposing the constraints by

$$\mathbf{0} = \mathbf{H}\mathbf{\Delta x} \tag{10}$$

which leads to a new constraint matrix $\mathbf{H} = (\mathbf{B}^T\mathbf{B})^{-1}\mathbf{B}^T$ with the dimensions $6 \times 3N$ which can be again used to generate a weighted regular datum matrix using the covariance matrix $\mathbf{\Sigma}$:

$$\mathbf{N}_H = \mathbf{H}^T\mathbf{\Sigma}^{-1}\mathbf{H}. \tag{11}$$

In both cases, so-called pseudo-observations are introduced and new regular NEQ systems are compiled (Eq. 12). Numerically, these two approaches should lead to the same results (Kotsakis 2012), however, the implementation of Eq. 11 is preferred due to better numerical stability. The NEQ systems of the pseudo-observations are then added to the NEQ of the real VLBI observations:

$$\mathbf{N} = \mathbf{N}_{free} + \mathbf{N}_{B/H}. \tag{12}$$

As further shown in Kotsakis (2012), the estimated parameters of the minimal constrained NEQ system are independent of the introduced covariance matrix from a mathematical point of view. However, the covariance matrix of the final NEQ system shows a dependency (see Eq. 13).

$$\mathbf{C}_{\mathbf{x},B/H} = \sigma^2(\mathbf{N}_{free} + \mathbf{N}_{B/H})^{-1}\mathbf{N}_{free}(\mathbf{N}_{free} + \mathbf{N}_{B/H})^{-1} \tag{13}$$

For more details, see Kotsakis (2012, 2013). Nevertheless, in the case of an over-constrained NEQ system, the choice of $\mathbf{\Sigma}$ has an impact on the estimated parameters (Kotsakis and Chatzinikos 2017).

To summarize, there are three possible approaches to introduce a terrestrial *geodetic datum*. For obvious reasons, we exclude the *3-2-1 method* where six coordinate components of three stations are simply fixed to their a priori value (Nothnagel 2023). First, by enlarging the datum-free normal equation matrix system with conditions (Helmert rendering, see Eq. 3) or second, by adding the squared and weighted

constraint matrix **B** (NNT/NNR, see Eq. 8) to the singular NEQ system or third, by using the discussed **H** (NNT/NNR, see Eq. 11).

3 Data

In the following, VLBI-only TRFs using the three different terrestrial datum realization methods are estimated based on two datasets:

- *dataset #1*: 24-hour sessions (1108 sessions, 66 stations, time frame: January 01 2015–December 31 2020)
- *dataset #2*: CONT17 legacy-1 sessions (15 sessions, 14 stations, time frame: November 28–December 12 2017) (Behrend et al. 2020)

Hence, the differences caused by the different datum methods imposed on a VLBI network over a short time frame can be compared to a combination of many global sessions over a longer time period. Furthermore, due to the longer time frame of *dataset #1*, station velocities are estimated using the transformation model extended by the rates of the datum parameters (Nothnagel 2023). It has to be stated here again, that typically, global solutions combine the data of thousands of VLBI sessions, however, the combination process is computationally expensive and the focus of the study is on highlighting the differences of the datum methods on the TRF determination rather than calculating highly precise reference frames. Thus, only the differences between the estimated station positions **dx** and their formal errors **mx** as well as between the estimated station velocities **dvx** and their formal errors **mvx** (in the case of *dataset #1)* are displayed in Sect. 4.

In this study, the list of datum stations is taken from the most recent VIE solution (Kraśná et al. 2023) in the case of both datasets. In Fig. 1, the station network of both experiments is displayed. The most recent ITRS realization, ITRF2020 (Altamimi et al. 2022), is selected as the a priori reference frame in the process of regularization and potential station position discontinuities have been adopted. Source positions are fixed to their ICRF3 position (Charlot et al. 2020). Furthermore, EOP, clocks and atmospheric parameters as well as baseline-dependent clock offsets (Krásná et al. 2021) are reduced session-wise. In general, by using the same input data for all solutions, the analysis directly shows the impact of the different datum realization methods on the TRF determination.

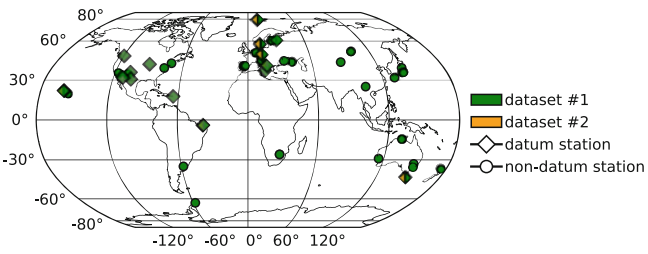

Fig. 1 Station networks of *dataset #1* (green) and *dataset #2* (orange). Datum stations are represented as diamonds, reduced stations as pentagons and remaining stations as circles. If a station occurs in both networks, the marker is split in two

4 Results

Since Helmert rendering is the strictest approach through application of conditions and since we routinely use this method in our VLBI single-session and multi-session analysis at VIE with the Vienna VLBI and Satellite Software (VieVS) (Böhm et al. 2018), these solutions are chosen as a reference and are compared to the two NNT/NNR approaches in the following.

In Figs. 2 and 3 the reference solution is compared to the NNT/NNR approach using the datum matrix from Eq. 8 and in Figs. 4 and 5 it is compared to the NNT/NNR method using the **H** from Eq. 11. As already mentioned, due to the differences in the magnitude of the elements of **B** and **H**, different formal errors must be introduced to achieve a comparable strength of datum realization. Therefore, a formal error of 10 mm has been incorporated in the NNT/NNR method using **B** and 1 mm when using **H**. When considering the rates of datum parameters, formal errors of 10 mm/yr and 1 mm/yr are introduced respectively. In both cases, the resulting differences of *dataset #1* are displayed on the left and those of *dataset #2* on the right of the following figures. No station velocities are estimated for *dataset #2*. Stations marked with a star are used to define the datum in the global adjustment.

As expected, no differences are visible in the estimated corrections to the a priori values shown in Fig. 2. Differences only show up in the formal errors of the coordinate components. Figure 3 shows comparable results with regard to the impact of the datum realization methods on the estimated station velocities and their formal errors. In general, the southern VLBI stations of *dataset #1* show significantly larger differences in formal errors **mx** and **mvx**, which may indicate that the selection of stations contributing to the datum realization is not optimal for the stations in the southern hemisphere, which is a well-known issue within the VLBI community.

When comparing the second NNT/NNR approach (see Figs. 4 and 5) with the reference solution, again no differences in the estimated corrections to the a priori values are visible. However, in this case, the formal errors **mx** and **mvx** are more uniform than in Figs. 2 and 3. This method seems to provide greater stability across all stations, which appears reasonable, as this method exhibits greater numerical stability. In general, by introducing tighter con-

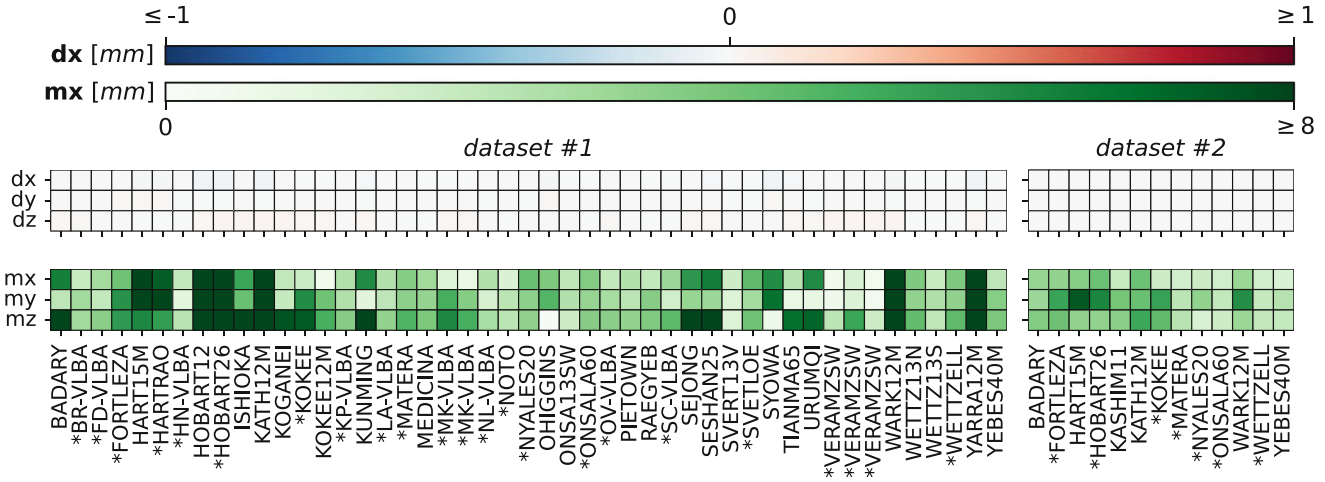

Fig. 2 Heatmap of differences in station coordinates **dx** and formal errors **mx** comparing the NNT/NNR approach using the **B** matrix and a formal error of 10 mm with the reference solution (Helmert rendering). The left column shows the results of *dataset #1* and the right column of *dataset #2*. Stations marked with a star are datum stations. The repeated listing of stations is due to discontinuities where each occurrence relates to a different interval

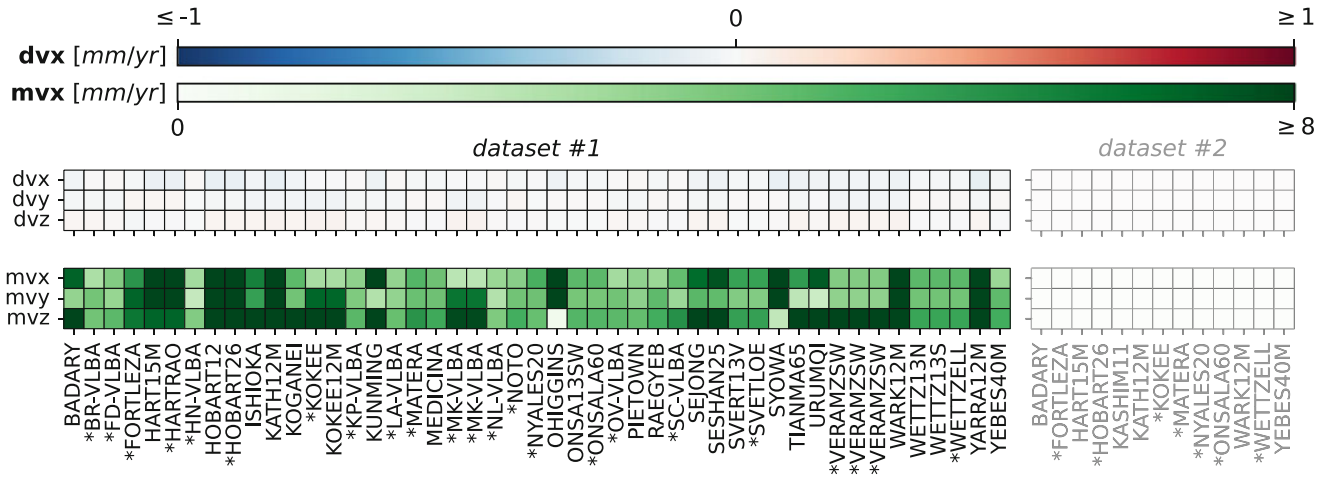

Fig. 3 Heatmap of differences in station velocities **dvx** and formal errors **mvx** comparing the NNT/NNR approach using the **B** matrix and a formal error of 10 mm/yr with the reference solution (Helmert rendering). The left column shows the results of *dataset #1*. No station velocities are estimated for *dataset #2*. Stations marked with a star are datum stations. The repeated listing of stations is due to discontinuities where each occurrence relates to a different interval

straints and therefore respectively increasing the weight of the constraints, the formal errors of the NNT/NNR method can be further decreased.

To sum up, the influence of the datum realization methods on the TRF solution depends on the selection of datum stations and the formal error chosen in the NNT/NNR approach. However, the covariance matrix of the constraints only influences the covariance matrix of the estimated parameters, and therefore their formal errors, and not the values themselves. Tighter constraints push the results towards those of the strict Helmert rendering conditions. The dependency of the formal errors of the estimated parameters in the case of minimal constraints on the chosen method and introduced formal errors makes the comparison of solutions a potential problem and demonstrates the importance of transparency in the VLBI community. To show the influence of the chosen formal error, the maximum absolute differences of the formal errors **mx** and **mvx** using the **H** matrix are presented in Table 1 which emphasizes that reducing the formal errors of the constraints pushes the results towards those of the Helmert rendering conditions.

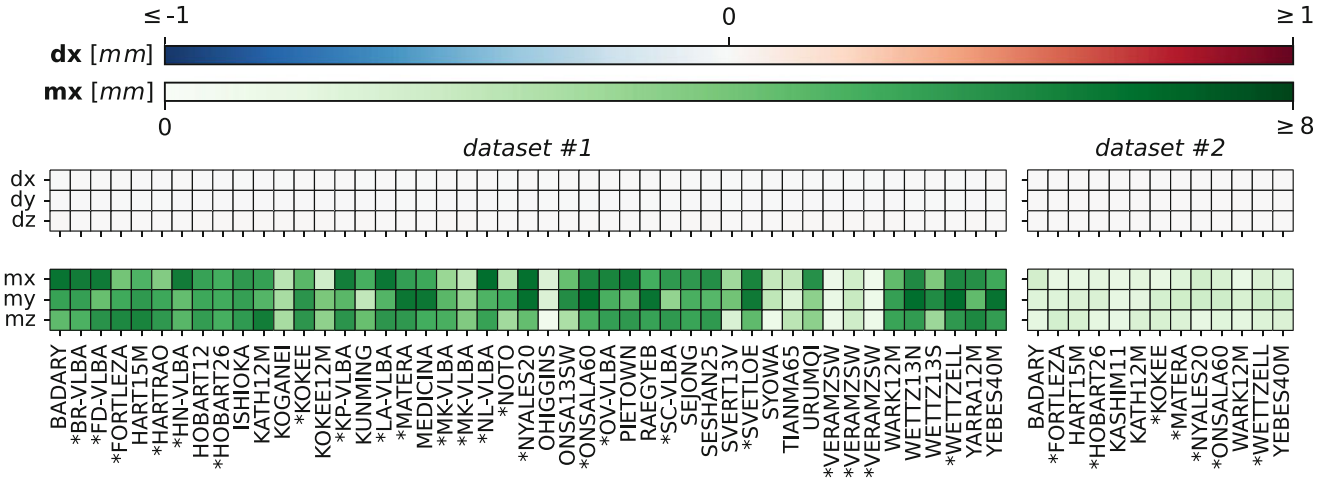

Fig. 4 Heatmap of differences in station coordinates **dx** and formal errors **mx** comparing the NNT/NNR approach using the **H** matrix and a formal error of 1 mm with the reference solution (Helmert rendering). The left column shows the results of *dataset #1* and the right column of *dataset #2*. Stations marked with a star are datum stations. The repeated listing of stations is due to discontinuities where each occurrence relates to a different interval

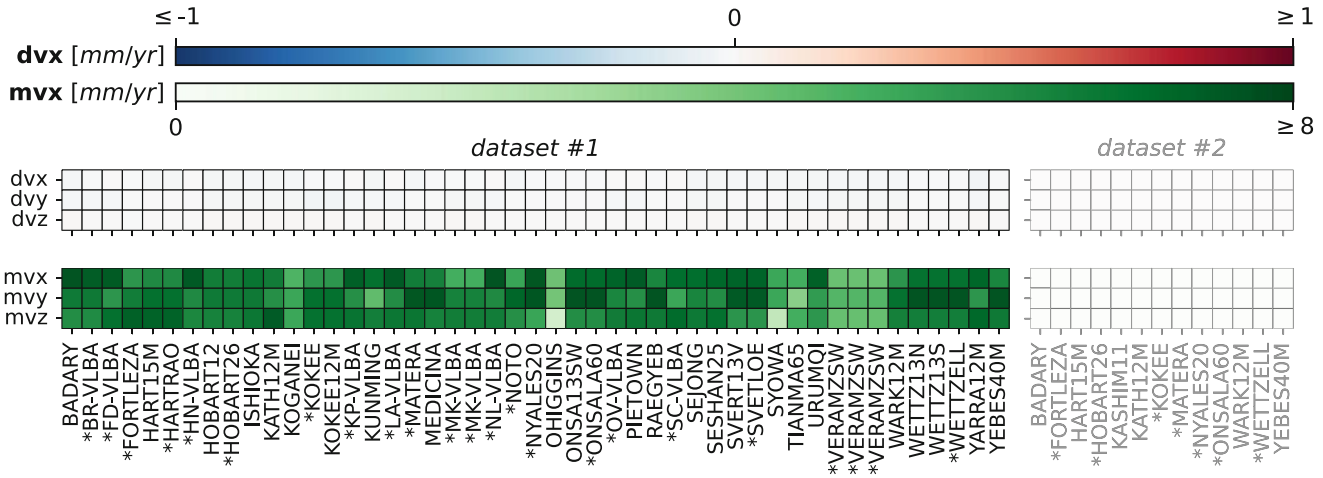

Fig. 5 Heatmap of differences in station velocities **dvx** and formal errors **mvx** comparing the NNT/NNR approach using the **H** matrix and a formal error of 1 mm/yr with the reference solution (Helmert rendering). The left column shows the results of *dataset #1*. No station velocities are estimated for *dataset #2*. Stations marked with a star are datum stations. The repeated listing of stations is due to discontinuities where each occurrence relates to a different interval

Table 1 Maximum absolute differences in the formal errors **mx** and **mvx** comparing the NNT/NNR approach using the **H** matrix and different formal errors for the datum constraints (values and rates) with the reference solution (Helmert rendering) given in mm. No station velocities are estimated for *dataset #2*

		Dataset #1		*Dataset #2*	
Formal error		**mx**	**mvx**	**mx**	**mvx**
1 mm	1 mm/yr	6.9	7.6	1.8	–
0.1 mm	0.1 mm/yr	0.3	0.5	0.1	–

5 Conclusion

The introduction of a *geodetic datum* is inevitable when analyzing VLBI sessions. Different methods of datum realization do not lead to significant differences in the computed TRFs when introducing minimal constraints. These findings are in agreement with the theoretical investigation by Kotsakis (2012). For both datasets, large differences in the formal errors of the estimated parameters of almost up to one cm between the methods can be seen when using a formal error of 10 mm (10 mm/yr) in the case of **B** and respectively 1 mm (1 mm/yr) in the case of **H**. This

indicates that tighter constraints need to be imposed in the NNT/NNR approach to achieve the same effect as when the Helmert rendering is performed. In general, the NNT/NNR method utilizing **H** is always preferable to using **B**. It not only demonstrated superior stability across all stations in the current investigation but is also considered more stable numerically. However, until now it is not reported by VLBI analysis centers which method and whether formal errors are applied to the datum constraints. This study aims to demonstrate the importance of transparency in the VLBI community, as comparing solutions, especially their variance information, can be problematic due to the use of different methods.

Acknowledgements We are grateful to all parties that contributed to the success of the CONT17 campaign. A detailed listing of all institutions is provided under https://ivscc.gsfc.nasa.gov/program/cont17/. We would like to thank the editor as well as Miltiadis Chatzinikos and an anonymous reviewer for the constructive comments and valuable suggestions.

Conflict of Interest The authors declare that they have no conflict of interest.

Authors' Contributions All authors designed the study. LK performed the evaluations and analysis. All authors worked on the theoretical considerations, discussed the results and contributed on the final manuscript.

References

Altamimi Z, Rebischung P, Collilieux X, et al (2022) ITRF2020: main results and key performance indicators. EGU General Assembly 2022 3958. https://doi.org/10.5194/egusphere-egu22-3958

Behrend D, Thomas C, Gipson J, et al (2020) On the organization of CONT17. J Geodesy 94(100). https://doi.org/10.1007/s00190-020-01436-x

Blaha G (1971) Inner adjustment constraints with emphasis on range observations. Department of Geodetic Science, The Ohio State University, OSU Report No. 148, Columbus

Böhm J, Böhm S, Boisits J, et al (2018) Vienna VLBI and Satellite Software (VieVS) for Geodesy and Astrometry. Publ Astron Soc Pac 130(986):044503. https://doi.org/10.1088/1538-3873/aaa22b

Charlot P, Jacobs CS, Gordon D, et al (2020) The third realization of the International Celestial Reference Frame by very long baseline interferometry. Astron Astrophys 644:A159. https://doi.org/10.1051/0004-6361/202038368

Dermanis A (1994) The photogrammetric inner constraints. ISPRS J Photogramm Remote Sens 49:25–39. https://doi.org/10.1016/0924-2716(94)90053-1

Kotsakis C (2012) Reference frame stability and nonlinear distortion in minimum-constrained network adjustment. J Geodesy 86:755–774. https://doi.org/10.1007/s00190-012-0555-6

Kotsakis C (2013) Generalized inner constraints for geodetic network densification problems. J Geodesy 87:661–673. https://doi.org/10.1007/s00190-013-0637-0

Kotsakis C, Chatzinikos M (2017) Rank defect analysis and the realization of proper singularity in normal equations of geodetic networks. J Geodesy 91:627–652. https://doi.org/10.1007/s00190-016-0989-3

Krásná H, Jaron F, Gruber J, et al (2021) Baseline-dependent clock offsets 287 in VLBI data analysis. J Geodesy 95(126). https://doi.org/10.1007/s00190-021-01579-5

Kraśná H, Baldreich L, Böhm J, et al (2023) VLBI celestial and terrestrial reference frames VIE2022b. Astron Astrophys 679:A53. https://doi.org/10.1051/0004-6361/202245434

Nothnagel A (2023) Elements of geodetic and astrometric very long baseline interferometry. Tech. rep., Technische Universität Wien, Austria. https://www.vlbi.at/data/publications/Nothnagel_Elements_of_VLBI.pdf

Sillard P, Boucher C (2001) A review of algebraic constraints in terrestrial reference frame datum definition. J Geodesy 75:63–73. https://doi.org/10.1007/s001900100166